Journal of Cardiovascular Magnetic Resonance 26 (2024) 100992

Contents lists available at ScienceDirect

Journal of Cardiovascular Magnetic Resonance

journal homepage: www.sciencedirect.com/journal/jocmr

Three-dimensional aortic geometry mapping via registration of non-gated contrast-enhanced or gated and respiratory-navigated MR angiographies

Lydia Dux-Santoy[a,*,1], Jose F. Rodríguez-Palomares[a,b,c,d,**,1], Gisela Teixidó-Turà[a,b,c], Juan Garrido-Oliver[a,d], Alejandro Carrasco-Poves[a,d], Alberto Morales-Galán[a], Aroa Ruiz-Muñoz[a,b], Guillem Casas[c], Filipa Valente[c], Laura Galian-Gay[b,c], Rubén Fernández-Galera[c], Ruperto Oliveró[c], Hug Cuéllar-Calabria[a,d,e], Albert Roque[a,d,e], Gemma Burcet[a,d,e], José A. Barrabés[a,b,c,d], Ignacio Ferreira-González[a,c,d,f,**], Andrea Guala[a,b]

[a] Vall d'Hebron Institut de Recerca (VHIR), Barcelona, Spain
[b] CIBER de Enfermedades Cardiovasculares, CIBER-CV, Instituto de Salud Carlos III, Madrid, Spain
[c] Department of Cardiology, Hospital Universitari Vall d'Hebron, Barcelona, Spain
[d] Departament of Medicine, Universitat Autònoma de Barcelona, Bellaterra, Spain
[e] Department of Radiology, Hospital Universitari Vall d'Hebron, Barcelona, Spain
[f] CIBER de Epidemiología y Salud Pública, CIBERESP, Instituto de Salud Carlos III, Madrid, Spain

ARTICLE INFO

Keywords:
Aortic aneurysm
Aortic dilation
Magnetic Resonance Angiography
Computer-assisted image processing
Aortic growth rate

ABSTRACT

Background: The measurement of aortic dimensions and their evolution are key in the management of patients with aortic diseases. Manual assessment, the current guideline-recommended method and clinical standard, is subjective, poorly reproducible, and time-consuming, limiting the capacity to track aortic growth in everyday practice. Aortic geometry mapping (AGM) via image registration of serial computed tomography angiograms outperforms manual assessment, providing accurate and reproducible 3D maps of aortic diameter and growth rate. This observational study aimed to evaluate the accuracy and reproducibility of AGM on non-gated contrast-enhanced (CE-) and cardiac- and respiratory-gated (GN-) magnetic resonance angiographies (MRA).

Methods: Patients with thoracic aortic disease followed with serial CE-MRA (n = 30) or GN-MRA (n = 15) acquired at least 1 year apart were retrospectively and consecutively identified. Two independent observers measured aortic diameters and growth rates (GR) manually at several thoracic aorta reference levels and with AGM. Agreement between manual and AGM measurements and their inter-observer reproducibility were compared. Reproducibility for aortic diameter and GR maps assessed with AGM was obtained.

Results: Mean follow-up was 3.8 ± 2.3 years for CE- and 2.7 ± 1.6 years for GN-MRA. AGM was feasible in the 93% of CE-MRA pairs and in the 100% of GN-MRA pairs. Manual and AGM diameters showed excellent agreement and inter-observer reproducibility (ICC > 0.9) at all anatomical levels. Agreement between manual and AGM GR was more limited, both in the aortic root by GN-MRA (ICC = 0.47) and in the thoracic aorta, where higher accuracy was obtained with GN- than with CE-MRA (ICC = 0.55 vs 0.43). The inter-observer reproducibility of GR by AGM was superior compared to manual assessment, both with CE- (thoracic: ICC = 0.91 vs 0.51) and GN-MRA (root: ICC = 0.84 vs 0.52; thoracic: ICC = 0.93 vs 0.60). AGM-based 3D aortic size and growth maps were highly reproducible (median ICC > 0.9 for diameters and > 0.80 for GR).

Abbreviations: AscAo, ascending aorta; AGM, aortic geometry mapping; CE-MRA, contrast-enhanced MRA; CMR, cardiovascular magnetic resonance; CTA, computed tomography angiography; DescAo, descending aorta; GN-MRA, electrocardiographic gated and respiratory navigated MRA; GR, growth rate; HD95, 95% Hausdorff distance; LoA, limits of agreement; MRA, magnetic resonance angiography; ICC, intra-class correlation coefficient

* Correspondence to: Cardiovascular Diseases, Vall d'Hebron Research Institute, Pg. de la Vall d'Hebron, 119-129, 08035 Barcelona, Spain.
** Correspondence to: Department of Cardiology, Hospital Universitari Vall d'Hebron, Pg. de la Vall d'Hebron, 119-129, 08035 Barcelona, Spain.
E-mail addresses: lydia.duxsantoy@vhir.org (L. Dux-Santoy), josefernando.rodriguez@vallhebron.cat (J.F. Rodríguez-Palomares), ignacio.ferreira@vallhebron.cat (I. Ferreira-González).
[1] Equal contributors and joint first authors.

https://doi.org/10.1016/j.jocmr.2024.100992
Received 4 December 2023; Accepted 21 December 2023

Conclusion: Mapping aortic diameter and growth on MRA via 3D image registration is feasible, accurate and outperforms the current manual clinical standard. This technique could broaden the possibilities of clinical and research evaluation of patients with aortic thoracic diseases.

Background

The cornerstone of the clinical management of patients with thoracic aorta aneurysms is the assessment of aortic diameters and their growth rate (GR) which, together with known cardiovascular risk factors, are used to guide treatment and to indicate prophylactic aortic surgery [1,2]. Thus, obtaining accurate and reproducible measurements of the aorta is of paramount importance for clinical decision making.

While transthoracic echocardiography is the first-line image modality in the evaluation of aortic root and proximal ascending aorta, computed tomography (CTA) or magnetic resonance (MRA) angiography are required to confirm echocardiographic measurements, especially when dilation is not confined to the proximal aorta [3]. Compared to MRA, CTA is often more available, faster and has higher spatial resolution, but exposes patients to ionizing radiation, which can be problematic in patients with frequent imaging. Thus, MRA is often preferred for imaging surveillance, especially in young patients. Various MRA techniques exist for aortic imaging [4]. Among them, contrast-enhanced MRA (CE-MRA) has been widely used. While providing marked contrast between the aorta and other structures, it needs contrast media and is often implemented without electrocardiographic (ECG) gating. This often results in motion artefacts that prevent proper assessment of the proximal aorta, which moves substantially during cardiac cycle [5]. To overcome these drawbacks, several contrast-free MRA sequences with ECG triggering and respiratory navigation (GN-MRA) have been introduced, showing excellent image quality and allowing accurate assessment of aortic diameters [4,6–10].

Current evaluation of aortic diameters and their growth is based on manual measurements performed perpendicular to the longitudinal axis of the aorta in a limited number of locations, localised through well-established anatomical landmarks [3]. This approach often precludes the identification of fastest dilation rates, rarely happening at these established locations [11], thus resulting in risk underestimation. Furthermore, the assessment of growth requires standardized serial measurements, which introduces further variability due to image obliquity and comparison of non-corresponding segments, among others [12]. While excellent reproducibility has been reported for manual aortic diameters in MRA [4,6,13–16], studies systematically evaluating the reproducibility of GR are lacking [17].

Recently, a novel technique to accurately quantify 3D aortic diameter and GR maps via deformable image registration of serial CTA has been presented [11,18], resulting in accurate and substantially more reproducible measurements than manual assessment [11]. However, the feasibility of this method once applied to MRA remains to be established. Thus, this observational study aimed to assess accuracy and inter-observer reproducibility of the aortic geometry mapping (AGM) technique applied to patients followed with CE- or GN-MRA compared to standard manual assessment.

Methods

Patient population

A retrospective search was performed to identify consecutive patients previously enrolled in research studies on aortic disease, free from aortic surgery and who underwent two or more MRA acquired at least 1 year apart between January 2010 and November 2021. MRA with artefacts preventing clinical assessment of aortic diameters were excluded. Both non-gated contrast-enhanced MRA (CE-MRA) and contrast-free ECG- and respiratory-navigated MRA (GN-MRA) were considered. The first 30 patients followed with serial CE-MRA and all 15 patients with serial GN-MRA follow-up were included. Six of the identified patients were followed both with CE-MRA and GN-MRA. The study was approved by the local ethics committee and patients signed an informed consent.

Magnetic resonance imaging

CE-MRA studies were acquired using different scanners (GE Signa HDxt 1.5 T, GE Healthcare, Waukesha, Wisconin and Siemens Avanto 1.5 T and Siemens Symphony 1.5 T, Siemens Healthineers, Erlangen, Germany) with 3D gradient echo sequences during breath-hold after the injection of a gadolinium-based contrast agent (0.15 mmol/kg gadobutrol at 3 mL/s) and timed according to the results of a bolus test technique. The typical acquisition time was 10–20 s

For the GN-MRA, a prospectively T2-prepared ECG-triggered segmented 3D TrueFISP (fast imaging with steady state precession) sequence was acquired during free breathing, using a motion-compensation diaphragm navigator (Siemens Symphony 1.5 T or Avanto 1.5 T). These acquisitions were performed without contrast injection or, in patients with both CE-MRA and GN-MRA, at the end of a comprehensive CMR protocol at least 20 min after contrast administration. Imaging acquisition times were between 4 and 10 min, depending on heart rate and respiratory motion.

Assessment of aortic diameters and growth rate

Two independent observers, blinded to each other's results, measured aortic diameters and their GR manually and with the AGM technique. The observers had 8 (observer 1) and 3 (observer 2) years of experience in cardiac imaging. Absolute aortic growth was calculated as the change in maximum diameter between follow-up and baseline scans, and divided by the years elapsed between scans to obtain GR. In patients with more than one follow-up MRA, each follow-up was compared with the same baseline MRA.

Manual measurements

Maximum thoracic aortic diameters were measured manually after double-oblique multiplanar reconstructions in the ascending (AscAo) and descending (DescAo) aorta at the level of the pulmonary bifurcation, and in the DescAo at the level of diaphragm, following the inner-to-inner edge convention, as recommended [3,19]. In patients followed with GN-MRA, cusp-to-cusp, cusp-to-commissure and maximum aortic root diameters were also assessed.

Aortic geometry mapping

Aortic diameter and GR maps were obtained semi-automatically using non-rigid image registration as described [11]. Briefly, the AGM technique involves the following steps (Fig. 1):

(i) Segmentation of the thoracic aorta and manual location of anatomical landmarks in the baseline MRA using 3D Slicer [20]. The supra-aortic vessels were included in the segmentation. Anatomical landmarks included: aortic annulus, sinotubular junction, brachiocephalic and left subclavian artery origins, diaphragm and pulmonary artery bifurcation. In GN-MRA, additional aortic root landmarks (mid-cusps and commissures) were identified.
(ii) Pre-processing of MRA studies and mesh generation. All acquisitions were manually cropped to the thoracic aorta region,

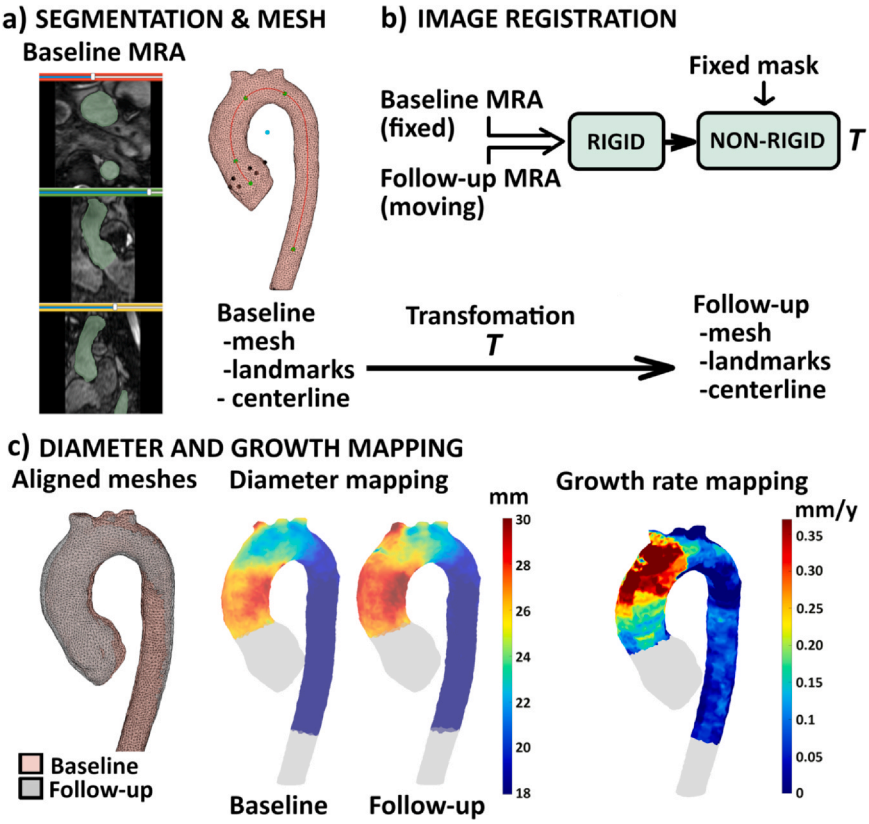

Fig. 1. Workflow to obtain 3D aortic geometry maps. (a) Manual segmentation of the thoracic aorta and location of anatomical landmarks. A 3D mesh is obtained and the centreline is calculated. (b) Alignment (rigid) and deformable (non-rigid) registration of baseline and follow-up images, identifying the transformation T. Follow-up mesh, landmarks and centreline are obtained by applying transformation T to their baseline counterparts. c) Local aortic diameters are automatically measured at each surface node at baseline and follow-up and used to calculate 3D maps. MRA: magnetic resonance angiography.

reoriented in the axial direction if needed and resliced to an isotropic voxel size of 0.75 mm. A 3D aortic mesh of at least 2500 nodes was obtained from the segmentation mask.

(iii) Multi-step intensity-based image registration using Elastix [21]. A rigid registration to align the previously cropped baseline and follow-up MRA, followed by a two-step multi-resolution non-rigid registration (affine and b-spline) using mutual information (within the 10 mm-thick regions of interest containing the aortic wall) and bending energy penalty (set to 50) [11] were performed. The overall transformation was applied to the baseline aortic mesh and landmarks to obtain their locations in the follow-up MRA. To evaluate the quality of the registration, the computed follow-up mesh was visualized overlaid on the follow-up MRA.

(iv) Thoracic aortic diameters and GR quantification using custom-designed Matlab software (The MathWorks Inc., Natick, Massachusetts, USA). Local thoracic aortic diameters were automatically measured at each surface node at baseline and follow-up and used to calculate GR, resulting in 3D maps of aortic diameters and GR. In GN-MRA, the distances between relevant aortic root reference points were used to measure diameter and GR. AGM measurements were extracted at the level of the different anatomical landmarks to be compared with manual assessment.

The code will be available at https://github.com/CardiovascularImagingVallHebron after external validation.

Statistics

Continuous variables were expressed as median and non-adjusted [1st–3rd] quartiles. Normality was assessed using the Shapiro–Wilk test. Inter-observer reproducibility of the manual baseline segmentations and the computed follow-up segmentations was assessed using the 95% value of Hausdorff distance (HD95). Correlation and Bland-Altman plots, Pearson correlation coefficient, and intra-class correlation coefficients (ICC) (single measures, two-way mixed, absolute agreement) were used to evaluate correlation and agreement between AGM and manual measurements, as well as the inter-observer reproducibility. To assess the accuracy of the AGM technique, the average of the observers' manual measurements was used. Pearson correlation and ICC values were considered: "excellent", for > 0.9; "good", between 0.75 and 0.9; "moderate", between 0.5 and 0.75, and "poor" for < 0.5. Statistical analysis was performed using Matlab (The MathWorks Inc., Natick, Massachusetts).

Results

Demographic variables, aneurysms aetiology, manually assessed aortic diameters and GR as well as details regarding gating and spatial resolution are reported in Table 1.

Among the 30 patients followed with CE-MRA, AGM was unsuccessful in 2 patients (6.7%), which were thus excluded from the study. A failure analysis suggested that failures were due to imprecise image registration due to deficient contrast-enhancement, blurring or poor edge sharpness and differences in fat suppression between the paired studies (Fig. S1). In the remaining 28 patients a total of 59 single CE-MRA scans and their corresponding 31 pairs were available for diameter and GR evaluation, respectively. Median follow-up was 3.3 years, ranging from 1.0 to 10.3 years and 3 patients had two follow-up studies. Conversely, all patients followed with GN-MRA had two scans, with a median follow-up of 2.2 years (ranging from 1 to 5.4 years), and AGM analysis presented no failures. In 6 patients, both CE- and GN-MRA were available.

Agreement between manual and AGM assessment of aortic diameters and GR, as well as inter-observer reproducibility for both techniques, are presented below for both CE- and GN-MRA. In the subgroup of patients followed with both MRA sequences, a comparison of the results is also reported.

Table 1
Demographic and clinical characteristics of the patients.

	CE-MRA patients		GN-MRA patients	
N	28		15	
Aetiology (N (%))				
Genetic syndrome	16 (57%)		13 (87%)	
Bicuspid aortic valve	8 (29%)		0 (0%)	
Degenerative	4 (14%)		2 (13%)	
Male sex (N (%))	13 (46%)		6 (40%)	
Age (y)	36.97 [21.31, 49.07]		20.69 [18.13, 42.99]	
Follow-up (y)	3.31 [2.06, 4.95]		2.16 [1.22, 4.34]	
	Baseline diameter (mm)	**GR (mm/year)**	**Baseline diameter (mm)**	**GR (mm/year)**
Aortic root (all)	-	-	35.52 [32.64, 38.65]	0.37 [0.15, 1.14]
Maximum	-	-	41.24 [38.14, 43.76]	0.40 [0.31, 0.85]
Cusp-to-cusp	-	-	34.72 [31.61, 37.20]	0.36 [0.12, 1.26]
Cusp-to-commissure	-	-	34.93 [32.63, 37.39]	0.45 [0.14, 0.95]
Thoracic aorta (all)	22.97 [20.06, 30.02]	0.24 [0.05, 0.40]	21.07 [17.68. 24.94]	0.33 [0.15, 0.57]
Ascending	33.30 [28.28, 40.06]	0.30 [0.17, 0.50]	28.75 [23.66, 31.32]	0.35 [0.16, 0.63]
Descending	21.89 [20.52, 25.80]	0.20 [0.09, 0.51]	18.92 [18.07, 22.63]	0.30 [0.14, 0.51]
Diaphragm	20.03 [18.90, 21.65]	0.21 [− 0.06, 0.34]	16.54 [15.47, 20.42]	0.32 [0.20, 0.57]
Characteristics of the sequences				
ECG-gating	No		Yes	
Respiratory-gating	No		Yes	
Pixel spacing (mm)	1.22 [1.03, 1.30]		0.78 [0.63, 0.80]	
Slice thickness (mm)	1.80 [1.50, 2.60]		0.90 [0.80, 2.00]	

Demographic and clinical characteristics of patients followed with contrast-enhanced (CE-) or ECG-gated and respiratory navigated (GN-) MRA. Manual measurements of aortic diameters and growth rates and key characteristics of the sequences are shown. MRA: magnetic resonance angiography.

Accuracy

Results of the accuracy of AGM measurements obtained both with CE- and GN-MRA are shown in Table 2 and Fig. 2. Detailed results at each measurement level and for each observer are reported in supplemental Tables S1, S2, S3 and S4 and Figs. S2 and S3.

In CE-MRA each observer assessed a total of 175 thoracic diameters and 91 GR (31 pairs of scans, diaphragmatic level was not acquired in one patient). In GN-MRA, each observer assessed 210 diameters and 105 GR in the aortic root and 90 diameters and 45 GR in the thoracic aorta.

AGM-based thoracic aorta diameters assessed either with CE- or GN-MRA presented excellent correlation ($R > 0.9$, Fig. 2A and B, respectively) and agreement (ICC > 0.9), and low bias (lower than spatial resolution) (Fig. 2C and D, respectively) compared to manual measures (Table 2), for both observers (Fig. S2). Agreement was excellent at all aortic levels, including the aortic root for GN-MRA (Table S3 and S4), and in both AscAo and DescAo for CE-MRA (Table S1 and S2). With

Table 2
Agreement between manual and AGM aortic diameters and growth rate assessed with CE-MRA and GN-MRA.

			AGREEMENT MANUAL-AGM	
CE-MRA		**N**	**Mean difference [LoA]**	**ICC [95% CI]**
THORACIC AORTA	**DIAMETER (mm)**	350	-0.27 [− 3.35, 2.81]*	0.983 [0.979, 0.986]*
	GROWTH RATE (mm/year)	182	0.21 [− 0.75, 1.17]*	0.431 [0.266,0.564]*
GN-MRA		**N**	**Mean difference [LoA]**	**ICC [95% CI]**
AORTIC ROOT	**DIAMETER (mm)**	420	-1.17 [− 4.42, 2.07]*	0.929 [0.791, 0.966]*
	GROWTH RATE (mm/year)	210	0.23 [− 0.91, 1.37]*	0.472 [0.320, 0.592]*
THORACIC AORTA	**DIAMETER (mm)**	180	-0.48 [− 2.83, 1.87]*	0.977 [0.963, 0.985]*
	GROWTH RATE (mm/year)	90	0.12 [− 0.76, 1.00]*	0.553 [0.389, 9683]*

Results of the comparison between manual (average of observers) and AGM (both observers). Mean difference, 95% limits of agreement (LoA) and intra-class correlation coefficient (ICC) with 95% confidence interval (CI) are shown. N is the number of comparisons. Symbol * refers to p-values < 0.05, indicating significance of the bias or of the ICC. AGM: aortic geometry mapping; ICC: intra-class correlation coefficient.

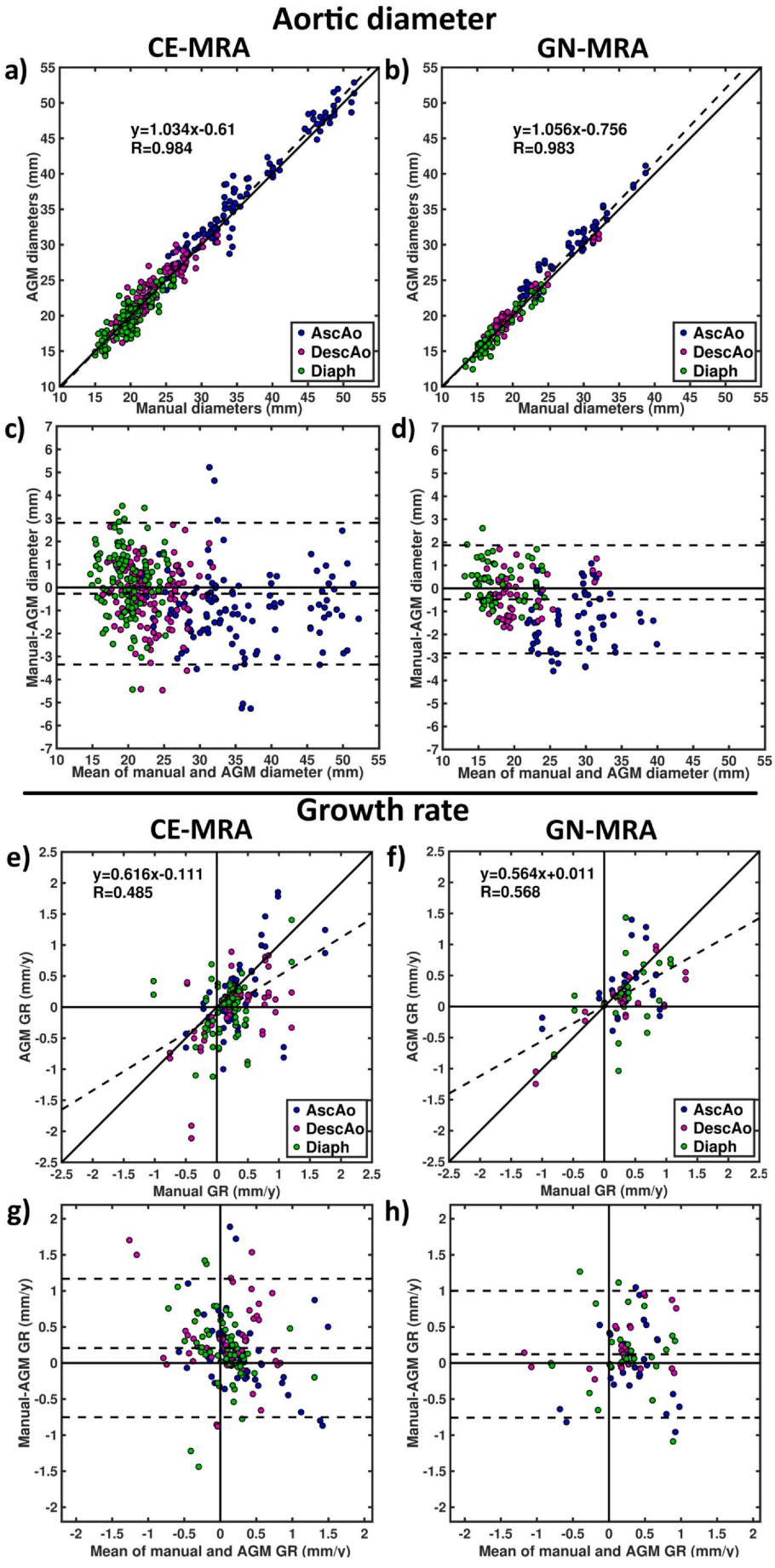

Fig. 2. Agreement between AGM and manual assessment of thoracic aorta diameters and growth rates. Correlation (A, B, E, F) and Bland-Altman plots (C, D, G, H) for AGM (both observers) compared to manual (average of observers) diameters (A-D) and growth rate (E-H) in patients followed with CE-MRA (A, C, E, G) and GN-MRA (B, D, F, H). Ascending (AscAo), descending (DescAo) and diaphragmatic (Diaph) aortic measurements are reported in blue, pink and green, respectively. Continuous lines represent bisectors (A, B, E, F) or zero (C, D, G, H), while dashed lines represent best linear fit (A, B, E, F) or mean and 95% confidence interval (C, D, G, H). AGM: aortic geometry mapping; CE-MRA: contrast-enhanced magnetic resonance angiography; GN-MRA: electrocardiographic gated and respiratory navigator gated magnetic resonance angiography.

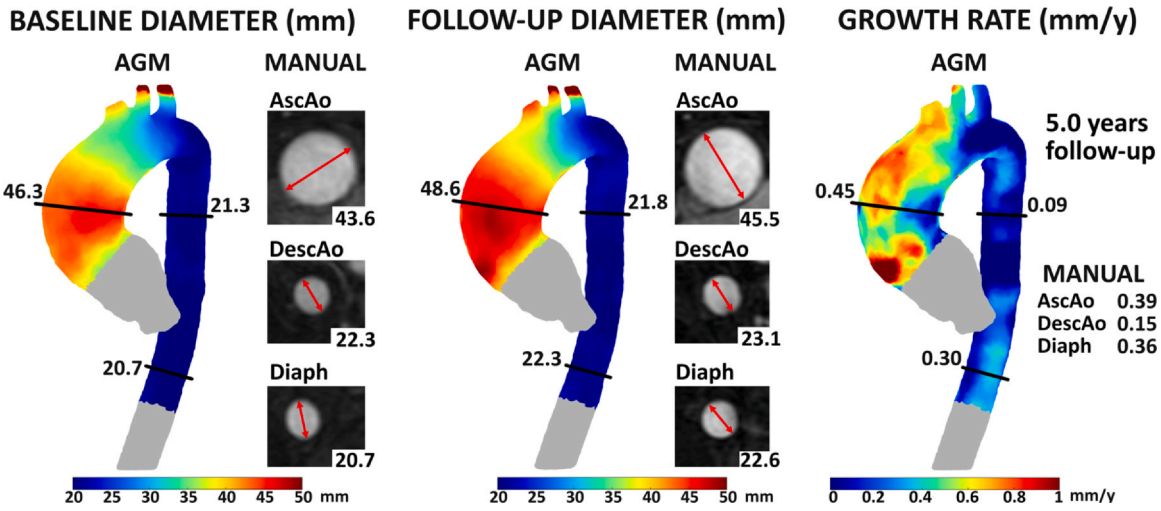

Fig. 3. Manual and AGM evaluation of aortic size in a patient with bicuspid aortic valve followed with CE-MRA. Mapping of baseline and follow-up aortic diameters and derived growth rate by AGM, together with manual and AGM maximum diameters and growth rate at the mid ascending (AscAo) and descending aorta (DescAo) and the diaphragmatic level (Diaph). AGM: aortic geometry mapping.

respect to aortic root measurements, bias between AGM and manual aortic root diameters was lowest for cusp-to-cusp measurements. An example of manual and AGM measurements obtained in a patient followed with CE-MRA is shown in Fig. 3.

Thoracic aorta GR demonstrated moderate correlation and agreement between AGM and manual measurements on GN-MRA (Fig. 2F, H) and more limited results for CE-MRA (Fig. 2E, G) for both observers (Fig. S3). The lowest accuracy was obtained at diaphragmatic level for CE-MRA (Tables S1 and S2) and at the AscAo for GN-MRA (Tables S3 and S4). In patients followed with GN-MRA, agreement for aortic root GR was limited, with slightly better accuracy for cusp-to-commissure compared to cusp-to-cusp measurements (Tables S3 and S4).

Reproducibility

Inter-observer reproducibility of the thoracic aorta segmentations, assessed by the HD95, was in the order of voxel size and was similar for the baseline (manually-segmented) meshes (HD95 = 1.81 [1.52, 2.18] mm for CE-MRA; 1.72 [1.49, 2.12] mm for GN-MRA) and the follow-up meshes obtained from registration (HD95 = 1.74 [1.44, 2.25] mm for CE-MRA; 1.67 [1.53, 2.18] mm for GN-MRA). Of note, a strong positive correlation was obtained between the HD95 of the baseline and follow-up meshes (r = 0.94 for CE-MRA, r = 0.98 for GN-MRA; $p < 0.0001$ both).

Regarding diameters, inter-observer reproducibility was excellent (ICC > 0.9, Table 3) both for manual and AGM, either with CE- (Fig. S4) or GN-MRA (Fig. S5), with similar performance at all levels (Table S5 and S6). Similarly, inter-observer reproducibility was excellent for aortic root diameters in GN-MRA, irrespectively of the measurement convention.

Regarding aortic GR, AGM showed superior reproducibility compared to manual assessment at all thoracic levels, both for CE- (Fig. 4A-D, Table S5) and GN-MRA (Fig. 4E-H, Table S6), showing higher correlation (Figs. 4A,B and 4E,F) and narrower limits of agreement (Figs. 4C,D and 4G,H). Reproducibility was also higher for AGM compared to manual for aortic root GR assessed with GN-MRA (Table 3),

Table 3
Inter-observer reproducibility for manual and AGM aortic diameters and growth rate.

			INTER-OBSERVER REPRODUCIBILITY			
			MANUAL (OBS 1-OBS 2)		AGM (OBS 1-OBS 2)	
CE-MRA		**N**	**Mean difference [LoA]**	**ICC [95% CI]**	**Mean difference [LoA]**	**ICC [95% CI]**
THORACIC AORTA	**DIAMETER (mm)**	175	-0.72 [− 3.23, 1.80]*	0.985 [0.965, 0.992]*	-0.78 [− 3.18, 1.61]*	0.987 [0.962, 0.993]*
	GROWTH RATE (mm/year)	91	-0.18 [− 1.07, 0.71]*	0.511 [0.321, 0.657]*	-0.03 [− 0.46, 0.41]	0.913 [0.871, 0.941]*
GN-MRA		**N**	**Mean difference [LoA]**	**ICC [95% CI]**	**Mean difference [LoA]**	**ICC [95% CI]**
AORTIC ROOT	**DIAMETER (mm)**	210	-0.17 [− 3.53, 3.19]	0.947 [0.93, 0.96]*	-0.95 [− 4.73, 2.83]*	0.924 [0.858, 0.954]*
	GROWTH RATE (mm/year)	105	0.29 [− 1.14, 1.72]*	0.518 [0.335, 0.657]*	0.01 [− 0.53, 0.54]	0.836 [0.767, 0.885]*
THORACIC AORTA	**DIAMETER (mm)**	90	-0.60 [− 2.63, 1.43]*	0.980 [0.949, 0.990]*	-0.80 [− 2.28, 0.67]*	0.985 [0.855, 0.995]*
	GROWTH RATE (mm/year)	45	-0.08 [− 1.00, 0.88]	0.595 [0.370, 0.754]*	0.04 [− 0.34, 0.40]	0.927 [0.871, 0.959]*

Mean difference, 95% limits of agreement (LoA) and intra-class correlation coefficient (ICC) with 95% confidence interval (CI) are shown for diameter and growth rate measurements. N is the number of comparisons. Symbol * refers to p-values < 0.05, indicating significance of the bias or of the ICC. AGM: aortic geometry mapping; CE-MRA: contrast-enhanced magnetic resonance angiography; GN-MRA: electrocardiographic triggered and respiratory navigator gated magnetic resonance angiography.

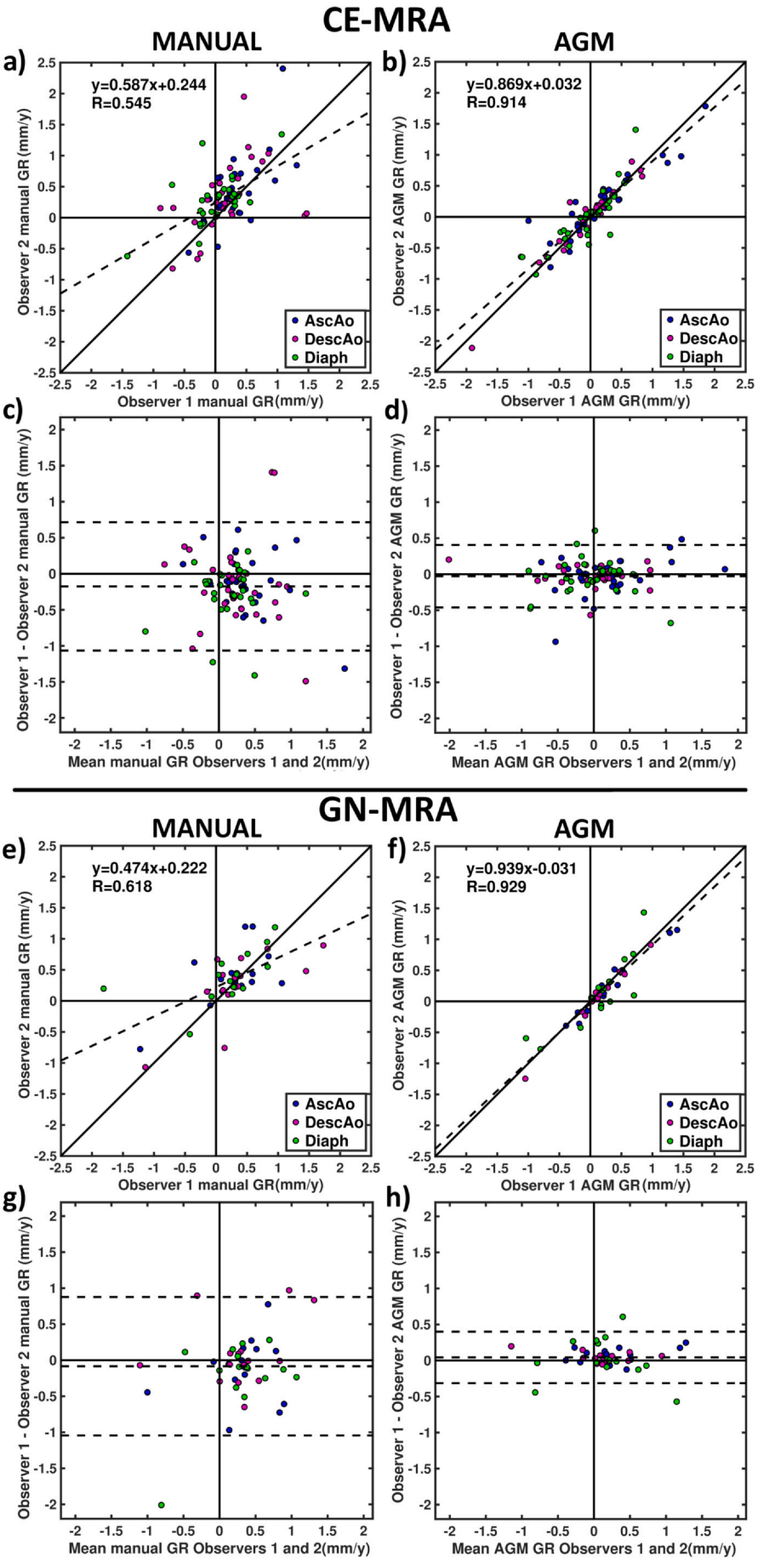

Fig. 4. Inter-observer reproducibility of thoracic aorta growth rate for manual and AGM assessments. Correlation and Bland-Altman plots for the inter-observer reproducibility of growth rate by manual (A, C, E, G) and AGM (B, D, F, H) assessment in patients followed with CE-MRA (a-d) and GN-MRA (e-h). Ascending (AscAo), descending (DescAo) and diaphragmatic (Diaph) growth rates are reported in blue, pink and green, respectively. Continuous lines represent bisectors (A, B, E, F) and zero, while dotted lines represent best linear fit (A, B, E, F) or mean and 95% confidence interval (C, D, G, H). AGM; aortic geometry mapping; CE-MRA: contrast-enhanced magnetic resonance angiography; GN-MRA: electrocardiographic triggered and respiratory navigator-gated magnetic resonance angiography.

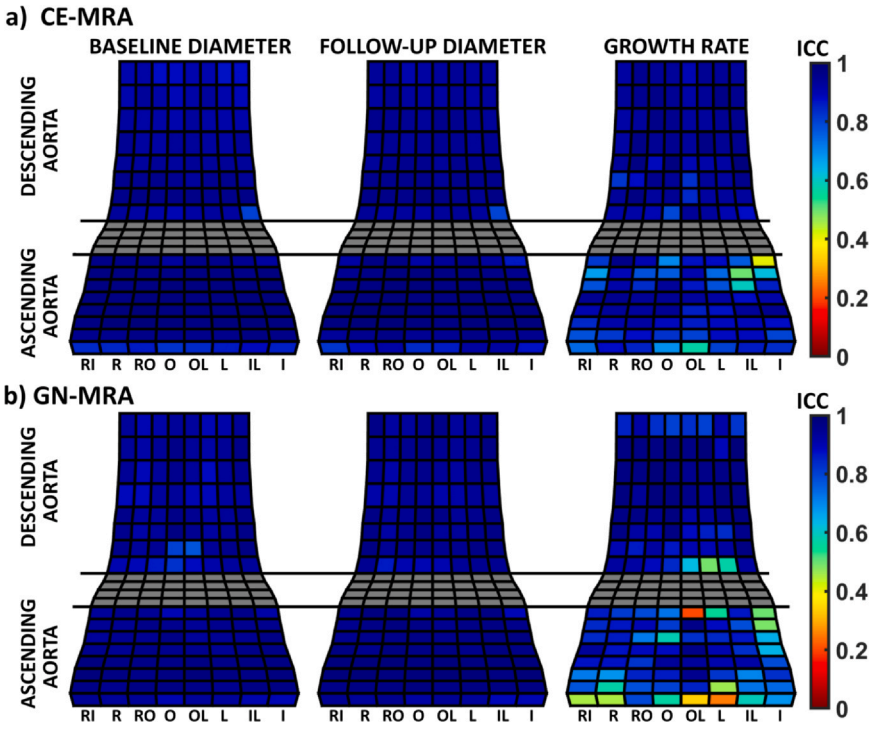

Fig. 5. Regional inter-observer reproducibility for thoracic aorta diameters and growth rate maps. Maps of intra-class correlation coefficient using (A) CE-MRA and (B) GN-MRA acquisitions for baseline and follow-up aortic diameters and growth rate. R, right; L, left; I, inner; O, outer; ICC, intra-class correlation coefficient. CE-MRA: contrast-enhanced magnetic resonance angiography; GN-MRA: electrocardiographic triggered and respiratory navigator-gated magnetic resonance angiography.

with cusp-to-cusp and cusp-to-commissure conventions resulting in higher reproducibility than maximum diameter (Table S6).

Aortic diameter and growth rate maps

Regional inter-observer reproducibility of AGM diameters and GR maps are shown in Fig. 5. The technique was able to assess regional baseline and follow-up diameters with excellent (ICC > 0.9) reproducibility at most regions, both for CE- and GN-MRA. Median regional ICC values were similar for CE- (0.97 AscAo, 0.93 DescAo) and GN-MRA (0.96 AscAo, 0.94 DescAo).

Inter-observer reproducibility for GR was mainly good (ICC > 0.75) in the AscAo and excellent (ICC > 0.9) in the DescAo, with similar results for CE- and GN-MRA. Median ICC in the AscAo and DescAo were 0.87 and 0.93 for CE-MRA and 0.82 and 0.94 for GN-MRA. Agreement was more limited (mainly moderate to good) in the proximity of the sinotubular junction and aortic arch.

Inter-sequence comparison

Results obtained with serial CE- and GN-MRA acquisitions were compared in the subgroup of 6 patients followed with both protocols. Measurements in the DescAo were excluded in one patient due to local registration failure attributable to the poor edge definition of the studies at this level.

Agreement between CE- and GN-MRA measurements at established landmarks was excellent for diameters and moderate for GR, both for manual (ICC = 0.976, bias [LoA] = 0.468 [−1.930,2.867] mm; ICC = 0.673, bias[LoA] = 0.080 [−0.903, 1.063] mm/year) and AGM (ICC = 0.984, bias[LoA] = −0.185 [−2.394, 2.023] mm; ICC = 0.708, bias[LoA] = 0.019 [−0.783, 0.820] mm/year). The inter-sequence agreement for GR was slightly better (lower bias and narrower LoA) for AGM compared with manual measurements.

Regional AGM measurements obtained with CE- and GN-MRA were discrepant in the most proximal AscAo, where the non-gated CE-MRA sequence showed poorer performance (Fig S5). After excluding this region, mid-to-distal AscAo and DescAo regional diameters showed excellent correlation and agreement between protocols (ICC = 0.973, bias[LoA] = −0.154 [−2.285, 2.542] mm, Fig S6 A and B), while agreement was moderate for GR (ICC = 0.583, bias[LoA] = 0.05 [−1.143, 1.243] mm/year, Fig S6 C and D). Inter-observer reproducibility of regional GR was slightly better for GN-MRA, which showed narrower limits of agreement than CE-MRA (bias[LoA] = −0.028 [−0.639, 0.582] mm/year) vs 0.042 [− 0.790, 0.873] mm/year).

Discussion

In the present work, an image registration technique (aortic geometry mapping, AGM), previously tested in CTA [11], was for the first time applied to serial 3D MRA to obtain 3D mapping of aortic diameters and growth rates. The main findings are:

(1) AGM-based thoracic aorta diameters at defined anatomic levels present excellent agreement with manual measurements and excellent inter-observer reproducibility both with CE- and GN-MRA.

(2) AGM-based thoracic aorta growth rates show limited agreement with manual assessment, both with CE- and GN-MRA. However, their inter-observer reproducibility was substantially higher compared to standard manual assessment. Similar results were obtained in the aortic root with GN-MRA.

(3) Using AGM 3D aortic maps of diameter and growth rate are feasible both with CE- and GN-MRA, showing mainly excellent reproducibility for regional diameters and good for growth rates. With GN-MRA, growth rate maps show better reproducibility and can also be obtained in the most proximal AscAo.

Manual assessment

In clinical practice, measurements of aortic diameters and growth are performed manually after multiplanar reformats at established anatomical landmarks [1,2]. This approach is subjected to multiple sources of variability, requires substantial time and allows to obtain a limited number of measurements [12]. In line with previous studies, this study showed that reproducibility is excellent for thoracic aorta diameters assessed either with CE- [4,8,22] or GN-MRA [4,6,13–16], and aortic root diameters with GN-MRA [4,13]. Also, diameters assessed with GN-MRA had slightly better inter-observer agreement than those assessed in CE-MRA, which is likely due to the better aortic edge

definition of this sequence [4,7,9,22], particularly in the most proximal aorta. Indeed, contrast-free ECG gated and navigated MRA sequences have shown to be comparable to contrast-enhanced CTA in terms of image quality and diameter [10,14,23].

Of note, this is the first study analysing inter-observer reproducibility for manual GR using MRA, which was moderate, highlighting the need for alternative techniques. Better results were found for GN-MRA, which further allowed to evaluate the aortic root. Reproducibility for manual GR assessment was higher in a previous study using CTA [11], an imaging modality with superior spatial resolution and more uniform arterial enhancement compared to MRA. However, it is worth noting that this improvement comes at the expense of radiation exposure.

Aortic geometry mapping

While several studies have proposed semi-automatic approaches to reduce time and variability in the assessment of aortic size using CTA [11,18,24–26], very few have tested similar strategies on MRA [27–29]. Previous studies have proposed calculating aortic diameter [27,28] or growth [29] from either manual or automatic aortic segmentations. The only previous publication evaluating 3D growth from MRA [29] proposed a rigid point-cloud registration of manually segmented baseline and follow-up aortae, followed by surface distance calculations to assess change between visits. In that work, while diameters correlated well with manual assessment, no comparison was presented for growth rates. A different approach based on deformable image registration has been recently applied to CTA [11,18], showing accurate and substantially more reproducible GR than manual assessment [11].

In line with that, AGM performed similarly to manual assessment for thoracic aorta diameters at standard anatomical landmarks, either with CE- or GN-MRA, with biases generally lower than the spatial resolution. For GR, AGM showed limited agreement with manual measurements but much better inter-observer reproducibility. The superior reproducibility of AGM-based GR and its limited agreement with manual measurements can be explained by the reduced observer dependency of the AGM approach, which is restricted to the segmentation of the aorta and identification of anatomical references in the baseline scan. The AGM technique further provides 3D maps of aortic diameter and GR, with mainly excellent inter-observer reproducibility for diameters and good for GR.

Of note, compared to findings in CTA [11], the agreement between AGM and manual GR measurements was lower, particularly for the non-gated MRA sequence. Conversely, although GR reproducibility was poorer in MRA than in CTA for manual assessment, it was comparable for AGM highlighting the robustness of the AGM technique.

Given its ability to measure local growth with superior reproducibility, AGM can enhance the capability to detect changes in aortic diameter, thus potentially improving clinical management. Notably, AGM allows to identify the largest diameter and GR at any location, which could be overlooked through manual assessment [11,30] potentially underestimating patient risk. Indeed, maximum AscAo and DescAo diameter and GR are rarely located at the level of the pulmonary bifurcation, the standard anatomical reference [11]. Furthermore, the assessment of high-quality local aortic growth can contribute to better clinical management and to expand the understanding of aneurysms physiopathology, as recently shown [31]. It is worth mentioning that the manual tasks involved in AGM are likely to be automated via machine learning algorithms [32], thereby further reducing observer variability and analysis time, which can help to make the technique more suitable for clinical use. Moreover, employing CMR in patient surveillance, rather than CT, may enable the evaluation of aortic flow dynamics and biomechanics [33,34], thereby offering indicators with potential for supplementary risk assessment to improve patient management.

Inter-sequence comparison

Prior works have compared the image quality and diameter but not GR measurements between CE- and GN-MRA [4,9,23,35]. Consistent with previous research, excellent inter-sequence agreement was found for diameters. However, the inter-sequence agreement was only moderate for GR, and slightly better for AGM than for manual assessment. Measurements were more discrepant in the most proximal AscAo, where the non-gated sequence yielded poorer results, likely because of the better local image quality of GN- compared to CE-MRA produced by the suppression of cardiac motion and breathing artefacts [4,7,8,35]. This result supports the advice of using gated sequences for proximal aortic size assessment.

Limitations

This is a single-centre retrospective study including a limited number of patients to validate the AGM technique in non-gated CE-MRA (n = 30) and native ECG-gated and respiratory-navigated MRA (n = 15), with only 6 patients available for inter-sequence comparison. Nonetheless, measurements were obtained at several aortic levels and by two independent observers, thus providing a relatively large number of data points for comparison. Patients with advanced aortic dilation were not well represented in the patient population, particularly in the GN-MRA group which mainly included young genetic patients. In the subgroup of patients who underwent both CE- and GN-MRA, the GN-MRA acquisition was performed at the end of the MRA protocol: the effects of residual contrast agent on these otherwise contrast-free images cannot be ruled out.

Conclusions

A semi-automatic registration-based assessment of aortic diameter and growth rate on MRA images outperforms the current clinical standard. When applied to cardiac and respiratory gated MRA, it enables the evaluation of the aortic root and proximal aorta without the requirement of contrast media. This technique broadens the possibilities of clinical and research assessments of thoracic aorta aneurysms status and evolution.

Ethics approval and consent to participate

The study was approved by the Vall d'Hebron Hospital ethics committee and patients signed an informed consent.

Consent for publication

Not applicable.

Funding

This study has been supported by funding from the Instituto de Salud Carlos III (projects PI19/01480, PI20/01727 and PI21/00448), the Spanish Ministry of Science, Innovation and Universities (RTC2019-007280-1), the Spanish Society of Cardiology (SEC/FEC-INV-CLI 20/015), and the Biomedical Research Networking Center on Cardiovascular Diseases (CIBERCV). Guala A. has received funding from "la Caixa" Foundation (LCF/BQ/PR22/11920008). Garrido-Oliver J. has received funding from Secretaria d'Universitats i Recerca del Departament de Recerca i Universitats de la Generalitat de Catalunya i del Fons Europeu Social Plus (AGAUR-FI 2023 FI-1 00322 Joan Oró).

CRediT authorship contribution statement

Ruperto Oliveró: Data curation, Validation, Writing – review & editing. **Hug Cuéllar-Calabria:** Data curation, Validation, Writing –

review & editing, Resources. **Lydia Dux-Santoy:** Conceptualization, Data curation, Formal analysis, Investigation, Methodology, Software, Supervision, Validation, Visualization, Writing – original draft, Writing – review & editing. **Jose F Rodríguez-Palomares:** Conceptualization, Funding acquisition, Investigation, Methodology, Supervision, Writing – review & editing, Validation. **Albert Roque:** Data curation, Validation, Writing – review & editing, Resources. **Gisela Teixidó-Turà:** Data curation, Funding acquisition, Investigation, Methodology, Supervision, Validation, Writing – review & editing, Conceptualization. **Gemma Burcet:** Data curation, Resources, Validation, Writing – original draft. **Juan Garrido-Oliver:** Formal analysis, Software, Validation, Writing – review & editing. **José A Barrabés:** Data curation, Validation, Writing – review & editing. **Alejandro Carrasco-Poves:** Investigation, Methodology, Validation, Writing – review & editing. **Ignacio Ferreira-González:** Formal analysis, Investigation, Resources, Validation, Writing – review & editing. **Alberto Morales-Galán:** Investigation, Methodology, Validation, Writing – review & editing. **Andrea Guala:** Conceptualization, Formal analysis, Investigation, Methodology, Software, Supervision, Validation, Writing – review & editing. **Aroa Ruiz-Muñoz:** Formal analysis, Investigation, Validation, Writing – review & editing. **Guillem Casas:** Data curation, Investigation, Validation, Writing – review & editing. **Filipa Valente:** Data curation, Validation, Writing – review & editing. **Laura Galian-Gay:** Data curation, Validation, Writing – review & editing. **Rubén Fernández-Galera:** Data curation, Validation, Writing – review & editing.

Data availability

The datasets generated and/or analysed during the current study are not publicly available due privacy issues but are available from the corresponding author on reasonable request. The code will be available at https://github.com/CardiovascularImagingVallHebron after external validation.

Declaration of Competing Interest

The authors declare that they have no competing interests.

Acknowledgements

The authors are grateful to Hannah Cowdrey for English revision and to Alicia Fresno for all her support.

Appendix A. Supporting information

Supplementary data associated with this article can be found in the online version at doi:10.1016/j.jocmr.2024.100992.

References

[1] Isselbacher EM, Preventza O, Hamilton Black III J, Augoustides JG, Beck AW, Bolen MA, et al. 2022 ACC/AHA guideline for the diagnosis and management of aortic disease. J Am Coll Cardiol 2022;80:e223–393.
[2] Erbel R, Aboyans V, Boileau C, Bossone E, Di Bartolomeo R, Eggebrecht H, et al. 2014 ESC guidelines on the diagnosis and treatment of aortic diseases: document covering acute and chronic aortic diseases of the thoracic and abdominal aorta of the adult. Eur Heart J 2014;35:2873–926.
[3] Evangelista A, Sitges M, Jondeau G, Nijveldt R, Pepi M, Cuellar H, et al. Multimodality imaging in thoracic aortic diseases: a clinical consensus statement from the European Association of Cardiovascular Imaging and the European Society of Cardiology working group on aorta and peripheral vascular diseases. Eur Hear J Cardiovasc Imaging 2023;24:e65–85.
[4] Potthast S, Mitsumori L, Stanescu LA, Richardson ML, Branch K, Dubinsky TJ, et al. Measuring aortic diameter with different MR techniques: Comparison of three-dimensional (3D) navigated steady-state free-precession (SSFP), 3D contrast-enhanced magnetic resonance angiography (CE-MRA), 2D T2 black blood, and 2D cine SSFP. J Magn Reson Imaging 2010;31:177–84.
[5] Guala A, Teixidó-Tura G, Rodríguez-Palomares JF, Ruiz-Muñoz A, Dux-Santoy L, Villalva N, et al. Proximal aorta longitudinal strain predicts aortic root dilation rate and aortic events in Marfan syndrome. Eur Heart J 2019;40:2047–55.
[6] Von Knobelsdorff-Brenkenhoff F, Gruettner H, Trauzeddel RF, Greiser A, Schulz-Menger J. Comparison of native high-resolution 3D and contrast-enhanced MR angiography for assessing the thoracic aorta. Eur Heart J Cardiovasc Imaging 2014;15:651–8.
[7] Bannas P, Groth M, Rybczynski M, Sheikhzadeh S, Von Kodolitsch Y, Graessner J, et al. Assessment of aortic root dimensions in patients with suspected Marfan syndrome: Intraindividual comparison of contrast-enhanced and non-contrast magnetic resonance angiography with echocardiography. Int J Cardiol 2013;167:190–6.
[8] Pennig L, Wagner A, Weiss K, Lennartz S, Huntgeburth M, Hickethier T, et al. Comparison of a novel Compressed SENSE accelerated 3D modified relaxation-enhanced angiography without contrast and triggering with CE-MRA in imaging of the thoracic aorta. Int J Cardiovasc Imaging 2021;37:315–29.
[9] Snel GJH, Hernandez LM, Slart RHJA, Nguyen CT, Sosnovik DE, van Deursen VM, et al. Validation of thoracic aortic dimensions on ECG-triggered SSFP as alternative to contrast-enhanced MRA. Eur Radiol 2020;30:5794–804.
[10] Pamminger M, Klug G, Kranewitter C, Reindl M, Reinstadler SJ, Henninger B, et al. Non-contrast MRI protocol for TAVI guidance: quiescent-interval single-shot angiography in comparison with contrast-enhanced CT. Eur Radiol 2020;30:4847–56.
[11] Dux-Santoy L, Rodríguez-Palomares JF, Teixidó-Turà G, Ruiz-Muñoz A, Casas G, Valente F, et al. Registration-based semi-automatic assessment of aortic diameter growth rate from contrast-enhanced computed tomography outperforms manual quantification. Eur Radiol 2022;32:1997–2009.
[12] Elefteriades JA, Mukherjee SK, Mojibian H. Discrepancies in measurement of the thoracic aorta: JACC review topic of the week. J Am Coll Cardiol 2020;76:201–17.
[13] Nussbaumer C, Bouchardy J, Blanche C, Piccini D, Pavon AG, Monney P, et al. 2D cine vs. 3D self-navigated free-breathing high-resolution whole heart cardiovascular magnetic resonance for aortic root measurements in congenital heart disease. J Cardiovasc Magn Reson 2021;23:65.
[14] Poskaite P, Pamminger M, Kranewitter C, Kremser C, Reindl M, Reiter G, et al. Self-navigated 3D whole-heart MRA for non-enhanced surveillance of thoracic aortic dilation: a comparison to CTA. Magn Reson Imaging 2021;76:123–30.
[15] Zhu C, Haraldsson H, Kallianos K, Ge L, Tseng E, Henry T, et al. Gated thoracic magnetic resonance angiography at 3T: noncontrast versus blood pool contrast. Int J Cardiovasc Imaging 2018;34:475–83.
[16] Yacoub B, Stroud RE, Piccini D, Schoepf UJ, Heerfordt J, Yerly J, et al. Measurement accuracy of prototype non-contrast, compressed sensing-based, respiratory motion-resolved whole heart cardiovascular magnetic resonance angiography for the assessment of thoracic aortic dilatation: comparison with computed tomography angiograp. J Cardiovasc Magn Reson 2021;23:7.
[17] Oladokun D, Patterson BO, Sobocinski J, Karthikesalingam A, Loftus I, Thompson MM, et al. Systematic review of the growth rates and influencing factors in thoracic aortic aneurysms. Eur J Vasc Endovasc Surg 2016;51:674–81.
[18] Burris NS, Bian Z, Dominic J, Zhong J, Houben IB, Van Bakel TMJ, et al. Vascular deformation mapping for CT surveillance of thoracic aortic aneurysm growth. Radiology 2022;302:218–25.
[19] Isselbacher EM, Preventza O, Black JH, Augoustides JG, Beck AW, Bolen MA, et al. 2022 ACC/AHA guideline for the diagnosis and management of aortic disease: a report of the American Heart Association/American College of Cardiology Joint Committee on Clinical Practice Guidelines. Circulation 2022;146:E334–482.
[20] Fedorov A, Beichel R, Kalpathy-Cramer J, Finet J, Fillion-Robin JC, Pujol S, et al. 3D Slicer as an image computing platform for the Quantitative Imaging Network. Magn Reson Imaging 2012;30:1323–41.
[21] Klein S, Staring M, Murphy K, Viergever MA, Pluim JPW. Elastix: a toolbox for intensity-based medical image registration. IEEE Trans Med Imaging 2010;29:196–205.
[22] Smith LR, Darty SN, Jenista ER, Gamoneda GL, Wendell DC, Azevedo CF, et al. ECG-gated MR angiography provides better reproducibility for standard aortic measurements. Eur Radiol 2021;31:5087–95.
[23] Pamminger M, Kranewitter C, Kremser C, Reindl M, Reinstadler SJ, Henninger B, et al. Self-navigated versus navigator-gated 3D MRI sequence for non-enhanced aortic root measurement in transcatheter aortic valve implantation. Eur J Radiol 2021;137:109573.
[24] Gao X, Boccalini S, Kitslaar PH, Budde RPJ, Tu S, Lelieveldt BPF, et al. A novel software tool for semi-automatic quantification of thoracic aorta dilatation on baseline and follow-up computed tomography angiography. Int J Cardiovasc Imaging 2019;35:711–23.
[25] Sedghi Gamechi Z, Bons LR, Giordano M, Bos D, Budde RPJ, Kofoed KF, et al. Automated 3D segmentation and diameter measurement of the thoracic aorta on non-contrast enhanced CT. Eur Radiol 2019;29:4613–23.
[26] Gao X, Boccalini S, Kitslaar PH, Budde RPJ, Attrach M, Tu S, et al. Quantification of aortic annulus in computed tomography angiography: Validation of a fully automatic methodology. Eur J Radiol 2017;93:1–8.
[27] Müller-Eschner M, Müller T, Biesdorf A, Wörz S, Rengier F, Kauczor H, et al. 3D morphometry using automated aortic segmentation in native MR angiography: an alternative to contrast enhanced MRA. Cardiovasc Diagn Ther 2014;4:80–7.
[28] Hepp T, Fischer M, Winkelmann MT, Baldenhofer S, Kuestner T, Nikolaou K, et al. Fully automated segmentation and shape analysis of the thoracic aorta in non-contrast-enhanced magnetic resonance images of the German National Cohort Study. J Thorac Imaging 2020;35:389–98.

[29] Subramaniam DR, Stoddard WA, Mortensen KH, Ringgaard S, Trolle C, Gravholt CH, et al. Continuous measurement of aortic dimensions in Turner syndrome: a cardiovascular magnetic resonance study. J Cardiovasc Magn Reson 2017;19:20.
[30] Ahmed Y, Nama N, Houben IB, van Herwaarden JA, Moll FL, Williams DM, et al. Imaging surveillance after open aortic repair: a feasibility study of three-dimensional growth mapping. Eur J Cardio-Thoracic Surg 2021;60:651–9.
[31] Guala A, Dux-Santoy L, Teixido-Tura G, Ruiz-Muñoz A, Galian-Gay L, Servato ML, et al. Wall shear stress predicts aortic dilation in patients with bicuspid aortic valve. J Am Coll Cardiol Img 2022;15:46–56.
[32] Garrido-Oliver J, Aviles J, Mejía-Córdova M, Dux-Santoy L, Ruiz-Muñoz A, Teixidó-Turà G, et al. Machine learning for the automatic assessment of aortic rotational flow and wall shear stress from 4D flow cardiac magnetic resonance imaging. Eur Radiol 2022;32:7117–27.
[33] Ruiz-Muñoz A, Guala A, Rodriguez-Palomares J, Dux-Santoy L, Servato L, Lopez-Sainz A, et al. Aortic flow dynamics and stiffness in Loeys–Dietz syndrome patients: a comparison with healthy volunteers and Marfan syndrome patients. Eur Hear J Cardiovasc Imaging 2022;23:641–9.
[34] Gil-Sala D, Guala A, Garcia Reyes ME, Azancot MA, Dux-Santoy L, Allegue Allegue N, et al. Geometric, biomechanic and haemodynamic aortic abnormalities assessed by 4D flow cardiovascular magnetic resonance in patients treated by TEVAR following blunt traumatic thoracic aortic injury. Eur J Vasc Endovasc Surg 2021;62:797–807.
[35] Krishnam MS, Tomasian A, Malik S, Desphande V, Laub G, Ruehm SG. Image quality and diagnostic accuracy of unenhanced SSFP MR angiography compared with conventional contrast-enhanced MR angiography for the assessment of thoracic aortic diseases. Eur Radiol 2010;20:1311–20.